Third International Conference on Sustainable Construction Materials and Technologies http://www.claisse.info/Proceedings.htm

Flexural Behaviour of Composite Girders Using FRP and Precast Ultra-High-Strength Fiber-Reinforced Concrete Slabs

S.V.T. Janaka Perera[1*], Hiroshi Mutsuyoshi[1] and Nguyen Duc Hai[2]

[1]*Saitama University, Japan*
[2]*Marshall University, USA*
[*]*Structural Material Laboratory, Dept. of Civil and Env. Eng., Saitama University, 255 Shimo Okubo, Sakura-ku, Saitama, 338-8570, janaka@mail.saitama-u.ac.jp, mutuyosi@mail.saitama-u.ac.jp,hguyen@njrati.org*

ABSTRACT

Fibre reinforced polymer (FRP) has recently been utilized in the construction of many pedestrian and road bridges due to its light weight, high specific strength, and corrosion resistance. Hybrid FRP (HFRP) beams optimize the combined use of carbon-fibre reinforced polymer (CFRP) and glass-fibre reinforced polymer (GFRP) in a single wide-flange beam section. This paper presents the development of composite girders using HFRP I-beams and precast Ultra-High Strength Fiber Reinforced Concrete (UHSFRC) slabs. A number of full-scale flexural beam tests were conducted using different slab dimensions with/without epoxy bonding between the slab and HFRP I-beam. Delamination failure was not observed in the compressive flange of the HFRP I-beam and the high tensile strength of CFRP in the bottom flange was effectively utilized with the addition of the UHSFRC slab on the top flange. The flexural stiffness of GFRP beams was improved by reinforcing the bottom flange with GFRP and CFRP plates.

Keywords. Composite Girder, Fibre Reinforced Polymer, Flexural Stiffness

INTRODUCTION

Fibre reinforced polymer (FRP) has recently been adopted in many pedestrian and road bridges due to its light weight, high specific strength, and corrosion resistance. Presently, a hybrid FRP (HFRP) beam for bridge girder applications is being developed. The HFRP beam is expected to find its application in severe corrosive environments or where lightweight rapid construction is required. The application of HFRP composites could also contribute to a reduction in both the life cycle cost (LCC) of the structure as well as its environmental load due to its low carbon dioxide emission [Sakai 2005 and Tanaka et al. 2006].

The HFRP beam optimizes the combined use of carbon fibre reinforced polymer (CFRP) and glass fibre reinforced polymer (GFRP) in a single wide-flange beam section (Hai et al. 2010). While CFRP has high tensile strength and stiffness, it is relatively expensive, whereas GFRP is comparatively less expensive; has less attractive mechanical properties are lower than those of CFRP. In a beam subjected to bending moment about the strong axis, the top and bottom flanges are subjected to high axial stress while the web is subjected to shear stress. In HFRP beams, the flanges are fabricated using a combination of CFRP and GFRP layers. On the other hand, the web is composed entirely of GFRP because it is not subjected to the same high stresses. Therefore, the HFRP beam utilizes the advantages of both CFRP and GFRP for strength, stiffness and economy.

Although the top flange of a HFRP beam does not utilize the tensile capacity of CFRP, the bottom flange utilizes the advantages of CFRP. In other words, the top flange of a HFRP beam is uneconomical. Also, due to manufacturing limitations it is impossible to produce a HFRP beam with a GFRP top flange and HFRP bottom flange. Hence, to improve the effectiveness of a GFRP beam, only the bottom flange needs be improved using GFRP or CFRP plates.

According to past studies, GFRP beams fail due to delamination of the top flanges [Hai et al. 2010 and Perera et al. 2012]. However, a past study has shown that a topping slab prevents the top flange delamination of GFRP beams due to compressive stress (Perera et al. 2012). Ultra high-strength fibre reinforced concrete (UHSFRC) is being used in topping slabs because it enables the use of smaller cross-sections and durability. Therefore, the purpose of this paper is to present the flexural behaviour of pultruded FRP beams with a topping slab. Precast UHSFRC was used for the topping slab.

FLEXURAL TEST OF HFRP-UHSFRC COMPOSITE GIRDERS

Materials. The HFRP I-beams were manufactured using the pultrusion process using the FRP layer composition shown in Table 1. The top and bottom flanges of the I-beam were composed of CFRP and GFRP in order to increase flexural strength and beam stiffness. The overall height of the HFRP beam was 250 mm and the flange width was 95 mm as shown in Fig. 1. The mechanical properties of CFRP and GFRP are listed in Table 1. The effective mechanical properties of the HFRP laminates obtained from the material tests are listed in Table 2. The average mechanical properties of UHSFRC are listed in Table 3.

Test variables. The test variables for the full-scale beam flexural tests are listed in Table 4. Five specimens with different dimensions for the UHSFRC slab were tested. The geometry of the test specimens and the dimensions of the beam cross-sections are shown in Figs. 2 and 3. The total length of each specimen was 3,500 mm with the flexural and shear spans at 1,000 mm as shown in Fig. 2. Timber stiffeners were installed using epoxy bonding at a spacing of 500 mm on both sides of the web to prevent web buckling. Different types of shear connectors including headed bolts with/without epoxy bonding and slab anchors were tested to investigate the composite/non-composite actions between the HFRP beam and the UHSFRC slab (Fig. 3). The spacing of headed bolts and slab anchors was determined from the shear connection tests to prevent premature bolt shear failure as shown in Fig. 4.

Table 1. Mechanical Properties of Materials

Parameters		CFRP 0°	GFRP 0/90°	GFRP ±45°	GFRP CSM[a]
Volume fraction (%)		55	53	53	25
Volume content (%)	Flange	33	17	41	9
	Web	0	43	43	14
Young's modulus (kN/mm^2)	E_{11}	128.1	25.9	11.1	11.1
	E_{22}	14.9	25.9	11.1	11.1
Shear modulus (kN/mm^2)	G_{12}	5.5	4.4	10.9	4.2
Poisson's ratio (mm/mm)	ν_{12}	0.32	0.12	0.58	0.31

[a] CSM = Continuous Strand Mat

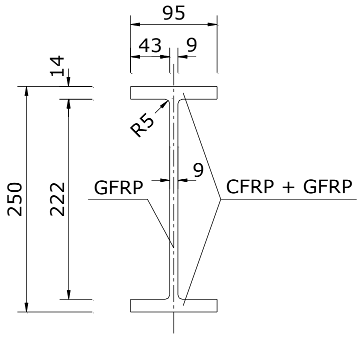

Figure 1. Dimensions of HFRP I-beams (unit: mm)

Table 2. Effective Mechanical Properties of HFRP Laminates

Property	Flange	Web
Compressive strength (N/mm^2)	394	299
Tensile strength (N/mm^2)	884	185
Young's modulus (kN/mm^2)	49.6	17.8

Table 3. Test Results of UHSFRC Material

Compressive strength (N/mm^2)	Tensile strength (N/mm^2)	Young's modulus (kN/mm^2)
173	14.3	48.6

Experimental setup and procedure. A four-point bending test was conducted on all specimens. The experimental setup is shown in Fig. 2. The load was applied by a manually-operated hydraulic jack until beam failure. The applied load, deflection at mid-span, and strains in the HFRP beam section were measured throughout the test.

Test results and discussion. Figure 5 shows the load and mid-span deflection relationship of each specimen. For comparison, the load-deflection relation curve for a HFRP beam without UHSFRC slab (control specimen) is also included in Fig. 5. All specimens with bolt shear connectors show higher stiffness and loading carrying capacity than the control specimen. In particular, the stiffness of specimen BE-135-50 is approximately 15% higher compared with that of specimen B-135-50. On the other hand, specimen SA-135-50 did not perform well compared to the specimens using headed bolts.

Table 4. Flexural Beam Test Variables

Specimen name	Shear Connector	EB[a]	W[b] (mm)	T[c] (mm)	EL[d] (mm)
B-135-50	M16 bolt	No	135	50	35
SA-135-50	Slab anchor M10	No	135	50	35
BE-95-50	M16 bolt	Yes	95	50	35
BE-135-35	M16 bolt	Yes	135	35	30
BE-135-50	M16 bolt	Yes	135	50	35

[a] EB = Epoxy bonding; [b] W = Width of UHSFRC slab;
[c] T = Thickness of UHSFRC slab; [d] EL = Embedded length of bolt

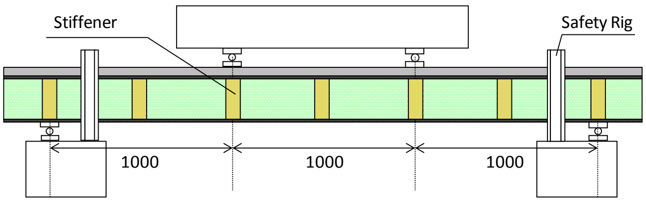

Figure 2. Geometry of specimen for flexural test (unit: mm)

All specimens with headed bolts failed due to crushing of the UHSFRC slab at the loading point followed by crushing of the HFRP beam flange as shown in Fig. 6a. Delamination of the top flange of the HFRP beam was observed in specimen SA-135-50 with shear anchors (Fig. 6b). This failure mode is similar to that of HFRP beams without a slab; however, the failure was not brittle as the UHSFRC slab carried compressive force even after delamination failure occurred. In addition, a few of the slab anchors failed in shear, while the others caused bearing failure in the HFRP beam flange.

Fibre model analysis of the HFRP-UHSFRC composite girders was conducted and the results were compared with the experimental results. Bernoulli-Euler theory was assumed in this analysis. A bi-linear stress-strain relationship from the design code for ultra-high-strength fibre reinforced concrete structures (Fig. 7) was used to model UHSFRC (Concrete Committee of JSCE 2004).

Table 5 shows comparisons between analytical and experimental results for the HFRP-UHSFRC composite girders that used headed bolt and epoxy bonding as shear connectors. The results indicated that the analytical model could well predict the failure load and failure mode of beams. The differences in failure load between the analysis and experiment are less than 5%. However, the analytical model over-estimates the stiffness of the composite girder as shown in Fig. 8.

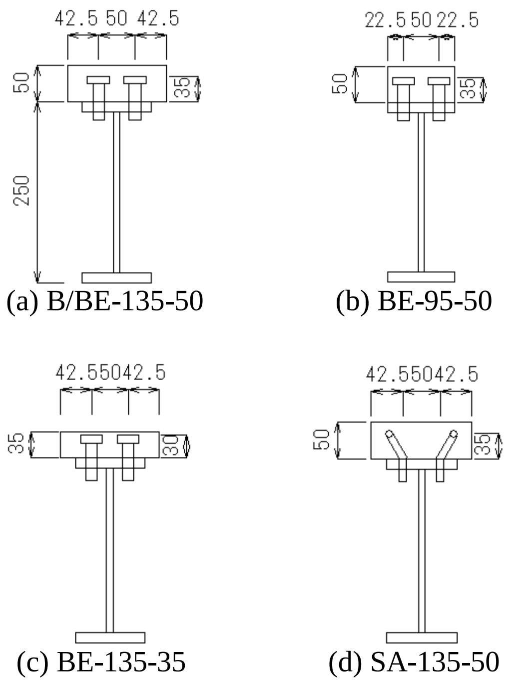

(a) B/BE-135-50 (b) BE-95-50

(c) BE-135-35 (d) SA-135-50

Figure 3. Dimensions of the beam cross-sections (unit: mm)

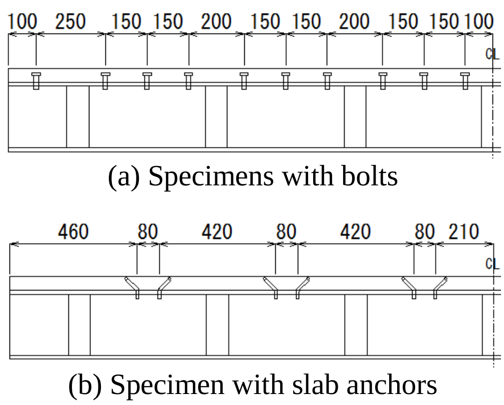

(a) Specimens with bolts

(b) Specimen with slab anchors

Figure 4. Locations of shear connectors (unit: mm)

According to the analytical model, compression failure of the UHSFRC slab should occur at mid-span. However, failure occurred at the loading point in the experiment and higher strains were recorded at the loading point due to stress concentration. The disagreement in stiffness between the analytical and experimental results is attributed in part to early plastic behaviour at the loading point caused by this stress concentration. The analytical model assumes perfect bond between the UHSFRC and HFRP, whereas the test specimens may experience some deformation at the bond interface.

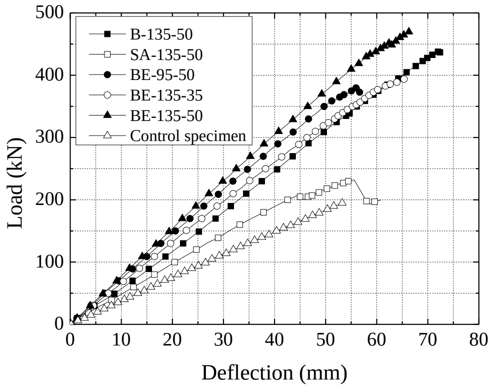

Figure 5. Load-deflection relationships

(a) Crushing of UHSFRC slab (b) HFRP flange delamination failure

Figure 6. Failure modes of composite girders in flexure

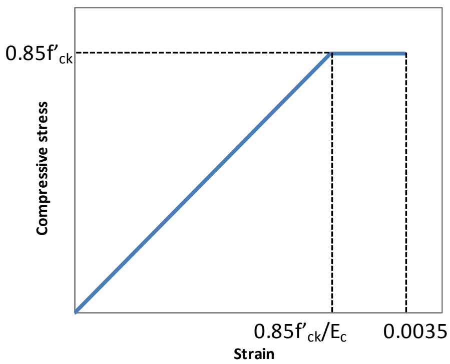

Figure 7. Bi-linear stress-strain relationship of UHSFRC

Table 5. Flexural Beam Test Results at Failure

Beam	Predicted failure load (kN)	Actual failure load (kN)	Predicted/actual failure mode
B-135-50	—	438	Compression (UHSFRC)
SA-135-50	—	232	Delamination (HFRP top flange)
BE-95-50	384	382	Compression (UHSFRC)
BE-135-35	411	394	Compression (UHSFRC)
BE-135-50	481	470	Compression (UHSFRC)

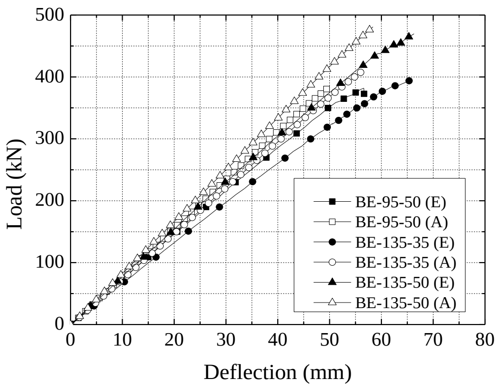

Figure 8. Comparisons of load-defection curves between experiments and analysis

FLEXURAL TEST OF REINFORCED FRP-UHSFRC COMPOSITE GIRDERS

Materials and Test variables. The overall height of the FRP I-beam was 250 mm and the flange thickness was 14 mm as shown in Fig. 9(a). The test variables for the beam flexural tests are listed in Table 6. Beams G-10, GG-10, GC-10, H-0, and H-10 were fabricated with precast UHSFRC segments (Fig. 9). Precast UHSFRC segments were installed using headed bolts and epoxy bonding. Beam G-only, without a topping slab, was used as the control specimen. The bottom flanges of beams GG-10 and GC-10 were reinforced using GFRP and CFRP plates respectively (Fig. 9(c)). The compressive strength, splitting tensile strength, and Young's modulus of UHSFRC were 173 MPa, 14.3 MPa, and 48.6 GPa respectively. Precast UHSFRC segments, with a length of 300mm were used for the topping slab and the segments were bonded using mortar and epoxy resin (Table 6). To study the effect of the UHSFRC-UHSFRC bonding method on FRP beams, two HFRP beams with topping slabs bonded using mortar (Beam H-10) and epoxy resin (Beam H-0) were tested (Table 6 and Fig. 9(d)).

Experimental setup and procedure. The beams were simply supported and tested in four-point bending at a span of 1250 mm with an interior loading span of 700 mm. The test setup is shown schematically in Fig. 10.

Test results and discussion. Fig. 11 shows the load and mid-span deflection relationship of the GFRP beams. For comparison, the load-deflection relation curve for a HFRP beam with UHSFRC slab, predicted using the fibre model (JSCE 2004) is also included in Fig. 11. The failure load of beam G-10 was 84% higher than that of beam G-only. This strength increase was due to the topping slab. The failure loads of beams G-10, GG-10, and GC-10 were approximately same. However, the deflection of beams GG-10 and GC-10 at the failure load was 28-30% lower than that of beam G-10. This reduction was due to the increase in the stiffness of beams GG-10 and GC-10. The load-deflection behaviour of beams GG-10 and GC-10 was similar and the deflection at the failure load was the same as that of the HFRP beam with the UHSFRC slab. In brief, flexural stiffness of GFRP beams (GG-10 and GC-10) was improved due to the reinforced bottom flange.

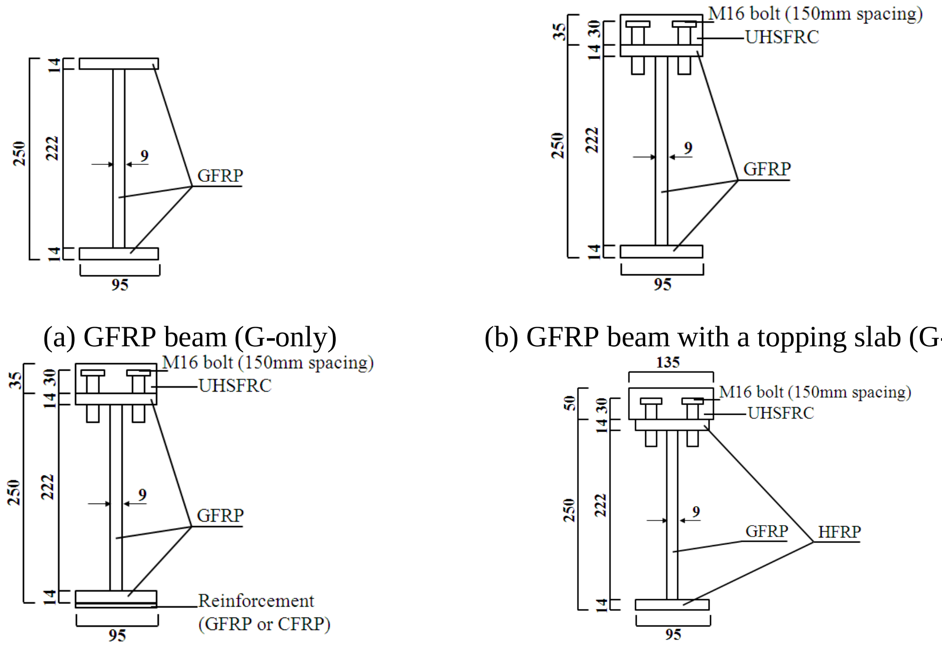

(a) GFRP beam (G-only)

(b) GFRP beam with a topping slab (G-10)

(c) Bottom reinforced GFRP beam with a topping slab (GG-10 and GC-10)

(d) HFRP beam with a topping slab (H-0 and H-10)

Figure 9. Dimensions of FRP I-beam (unit: mm)

Fig. 12 shows the load and mid-span deflection relationship of HFRP beams. The failure loads of beams H-0 (380kN) and H-10 (369kN) were approximately same. However, the straightness of beam H-10 was slightly lost at about 210kN. This straightness loss could be due to the failure of the mortar bonding of the topping slab at about 210kN.

Table 6. Test Variables for Reinforced FRP-UHSFRC Composite Girders

Specimen	Beam type	UHSFRC spacing	UHSFRC bonding method	Bottom flange thickness (mm)	Reinforcement
G-only	GFRP	10	Mortar	14	-
G-10	GFRP	10	Mortar	14	-
GG-10	GFRP	10	Mortar	14+8	GFRP plate
GC-10	GFRP	10	Mortar	14+1.2	CFRP plate
H-0	HFRP	0	Epoxy resin	14	-
H-10	HFRP	10	Mortar	14	-

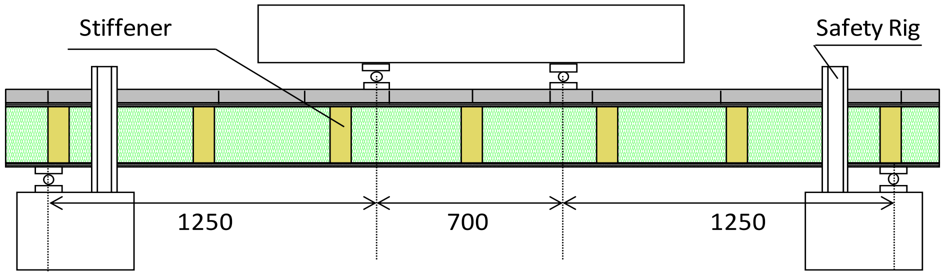

Figure 10. Geometry of specimen for flexural test (unit: mm)

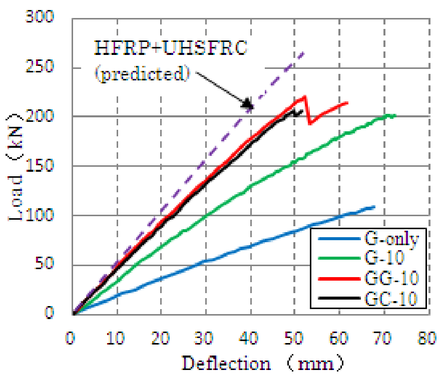

Figure 11. Load-deflection relationship of GFRP beams

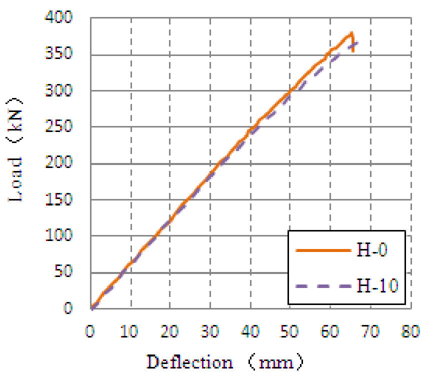

Figure 12. Load-deflection relationship of HFRP beams

Fibre model analysis of GFRP beams with a UHSFRC topping slab was conducted and the results were compared with the experimental results. A bi-linear stress-strain relationship from the JSCE design code was used to model UHSFRC (JSCE 2004) (Fig. 7). The difference in failure load between the analysis and experiment was less than 15% as shown in Fig. 13.

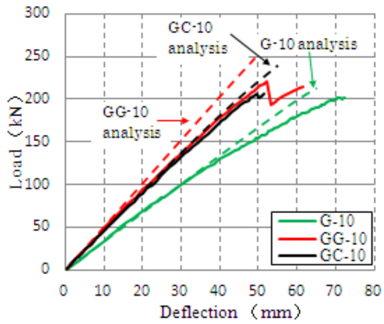

Figure 13. Comparison of load-deflection curves between experimental and analytical data

CONCLUSIONS

This paper presents an experimental study of composite girders consisting of FRP beams and concrete topping slabs connected by bolts or slab anchors. The main conclusions from the study are summarized as follows:

1. Composite girders consisting of HFRP beams and concrete topping slabs significantly improve their flexural stiffness and effectively utilize the superior properties of the HFRP materials.

2. Composite girders with epoxy bonding between the UHSFRC slab and HFRP beam top flange showed an approximate 15% increase in flexural stiffness than beams connected with bolts only.

3. The flexural stiffness of GFRP beams was improved by reinforcing the bottom flange with GFRP and CFRP plates. Therefore, the deflection of GFRP beams with a reinforced bottom flange at the failure load was 28-30% lower than that of the GFRP beam.

REFERENCES

Concrete Committee of Japan Society of Civil Engineers (JSCE) (2004). “Recommendations for Design and Construction of Ultra High Strength Fiber Reinforced Concrete Structures.” *JSCE Guidelines for Concrete*, No. 9, pp. 1-106.

Hai, N.D., Mutsuyoshi, H., Asamoto, S., and Matsui, T. (2010). “Structural Behavior of Hybrid FRP Composite I-Beam.” *Journal of Construction and Building Materials*, Vol. 24, pp. 956-969.

Perera, S.V.T.J., Mutsuyoshi, H., and Tomoya, A. (2012). “Development of Composite Beams Using Ultra-High Performance Fiber Reinforced Concrete and Fiber Reinforced Polymers.” *Proc. of JSCE 14th International Summer Symposium*, CD-ROM, Nagoya, Japan.

Sakai, K. (2005). “Environmental Design for Concrete Structures.” *Journal of Advanced Concrete Technology*, Vol.3, No.1, pp.17-28.

Tanaka, H., Tazawa, H., Kurita, M., and Shimomura, T. (2006). “A Case Study on Life-Cycle Assessment of Environmental Aspect of FRP Structures.”, *Proceedings of Third International Conference on FRP Composites in Civil Engineering* (CICE 2006), Florida, USA, pp. 175-178.